Lloyd's mirror effect in fin whale calls and its use to infer the depth of vocalizing animals

Andreia Pereira, Danielle Harris, Peter Tyack, and Luis Matias

Citation: Proc. Mtgs. Acoust. **27**, 070002 (2016); doi: 10.1121/2.0000249

View online: https://doi.org/10.1121/2.0000249

View Table of Contents: http://asa.scitation.org/toc/pma/27/1

Published by the Acoustical Society of America

Proceedings of Meetings on Acoustics

Volume 27 http://acousticalsociety.org/

Fourth International Conference on the Effects of Noise on Aquatic Life

Dublin, Ireland
10-16 July 2016

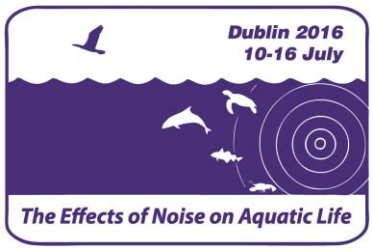

Lloyd's mirror effect in fin whale calls and its use to infer the depth of vocalizing animals

Andreia Pereira
Instituto Dom Luiz, Faculty of Sciences, University of Lisbon, Lisbon, Lisbon, Portugal
andreiafspereira@gmail.com

Danielle Harris
Centre for Research into Ecological and Environmental Modelling, University of St. Andrews, St. Andrews, Fife, United Kingdom
dh17@st-andrews.ac.uk, len.thomas@st-andrews.ac.uk

Peter Tyack
Sea Mammal Research Unit, University of St Andrews, St. Andrews, Fife, United Kingdom; plt@st-andrews.ac.uk

Luis Matias
Instituto Dom Luiz, Faculty of Sciences, University of Lisbon, Lisbon, Lisbon, Portugal; lmatias@fc.ul.pt

The ocean acoustic Lloyd's Mirror effect (LME) is produced by interference between the direct-path and the sea surface phase-reversed reflection of a sound as observed at a receiver. It results in a frequency-dependent interference pattern that can be observed in a spectrogram. Many studies have found variations of spectral characteristics of the 20 Hz 'regular' fin whale call, which seem to reflect geographic differences. However, variability of spectral measurements may occur due to the LME. Using a bout of regular calls with estimated ranges, our study aimed to: 1) show and analyze differences of call features due to the LME; and 2) estimate the depth of the vocalizing whale. The composite spectrogram showed that different spectral characteristics of the calls could be identified within the same bout. We developed transmission loss models considering the LME for a fin whale call generated close to the surface and recorded at the sea bottom by an instrument. Our results suggested that some differences measured in fin whale calls could be related to the LME. Inference of depths of calling whale was not straightforward and needed to be assessed at a finer temporal scale than the full bout of calls.

Published by the Acoustical Society of America

 [DOI: 10.1121/2.0000249]

1. INTRODUCTION

The acoustic repertoire of large cetaceans is differentiated at species and population levels, which can be useful for management purposes (McDonald et al., 2006). Some calls are highly stereotyped and are produced in repeated sequences, which aids automated sound detection. Fin whales produce calls between 15 and 142 Hz (Watkins et al., 1987; Hatch & Clark, 2004), but the most common and best studied call is the "20-Hz call" (hereafter regular call) (Hatch & Clark, 2004). This signal is a ~1 second, downward sweeping tone between 30 and 15 Hz (Watkins et al., 1987). Usually fin whales produce sequences of regular calls that are separated by two types of periods of silence: rests, which can last between 1–20 minutes, and longer gaps, lasting between 20 minutes and 2 hours (Watkins et al., 1987; Delarue et al., 2009; Soule & Wilcock, 2012). These sequences form bouts that are separated by periods of silence greater than 2 hours. Other types of low frequency sounds, such as back-beats, can be produced within sequences (Clark et al., 2002). Back-beats are relatively constant in frequency (between 18 and 20 Hz) and last ~0.8 second (Clark et al., 2002). Several studies have found variation in some temporal (e.g., inter-call interval, call duration) and spectral features of the regular call (e.g. frequency bandwidth, median frequency) that seem to reflect geographic differences (Hatch & Clark, 2004; Delarue et al., 2009; Castellote et al., 2011). However, variability of call measurements may also be caused by acoustic interference. When a sound source emits a signal, the pressure waves can travel through both direct and reflected paths (in water, signals can reflect off both the seafloor bottom and sea surface). Depending on sea state and signal frequency, the ocean surface can generate a reflected pressure signal with the phase reversed by 180 degrees. The interference between the direct path and this surface reflected signal is called the Lloyd's Mirror effect (hereafter LME) by analogy with optical interference. This results in alternating signal peaks caused by constructive interference, with signal nulls, caused by partial or complete cancellation. The LME is more prominent within the interference field, which is limited by the following ranges (Etter, 2013) that are a function of the source depth, Z_S, receiver depth, Z_R, and signal wavelength, λ:

$$Lower\ \ range\ limit \approx 2\sqrt{Z_s Z_r} \tag{1}$$

$$Higher\ \ range\ limit \approx \frac{4\pi \cdot Z_S Z_R}{\lambda} \tag{2}$$

For a shallow source (100 m) and an acoustic sensor at 4000 m, the lower and upper ranges estimated by these expressions are 1250 and 67,000 m, respectively, considering a 20 Hz monochromatic wave. Since the particle displacement is free at the ocean surface, the reflected displacement and velocity signal (which are those recorded by geophones in a seismometer) will have the same polarity as the direct signal, but the pressure signal recorded by a hydrophone will be phase-reversed. As a consequence, hydrophone and geophone recordings will show different interference patterns. The sea bottom also generates a reflected signal but we will not consider its effect. Ocean-bottom seismometers (OBS) record pressure and particle velocity at a location that is essentially at the sea bottom for low frequencies. Therefore, the effect of the surface reflection is expected to dominate. The surface reflection will affect the time and frequency structure of signals, thus changing the expected acoustic signal. This is evident in spectrograms where frequency-dependent interference patterns can be observed. Although the tendency of the LME to affect time/frequency measurements of acoustic signals may be detrimental to some analyses, it can also provide opportunities to obtain data. The LME can be used to provide an estimate of either

source depth or range from a receiver, if an *a priori* estimate of one of these variables is available. Using a sample of regular fin whale calls recorded by one OBS and with estimated ranges from the receiver, our study aimed to: 1) show and analyze differences of call features due to the LME; and 2) estimate the depth of the vocalizing whale.

2. METHODS

A. RECORDING INSTRUMENTS & DATASET

Between August 2007 and July 2008, 24 OBSs were deployed southwest of Portugal to study potential tsunami sources (Fig. 1). During this time, fin whale calls were also recorded, which have been the target of various studies (Harris et al., 2013; Matias & Harris, 2015). Depths of the recording instruments ranged from 1993 m to 5100 m. A description of the deployment, data recorded, and details about the instruments can be found in Harris et al. (2013).

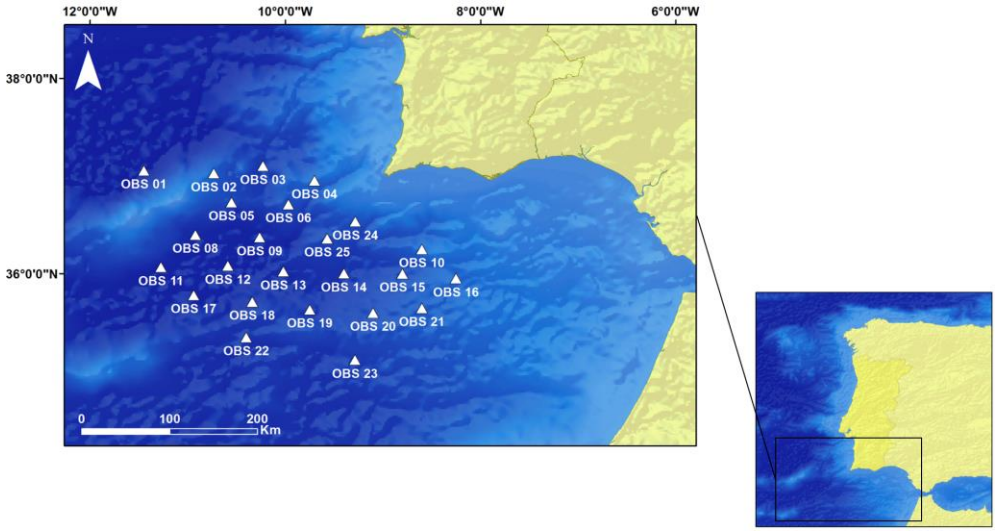

Figure 1. Location of the seismic monitoring array off southwest of Portugal.

We only considered the regular call type in this study. Bouts of regular fin whale calls were viewed as spectrograms that were calculated with TRITON (Wiggins, 2010), a software package written in MATLAB (Mathworks, 2010). During visual exploratory data analysis of these bouts, we noticed high signal-to-noise ratio calls with different spectral features. We hypothesized that these differences could be the result of surface interference. One bout was selected and analyzed in more detail (taken from OBS12, on November 9th 2007, between 01:00 and 03:00) (Fig. 2).

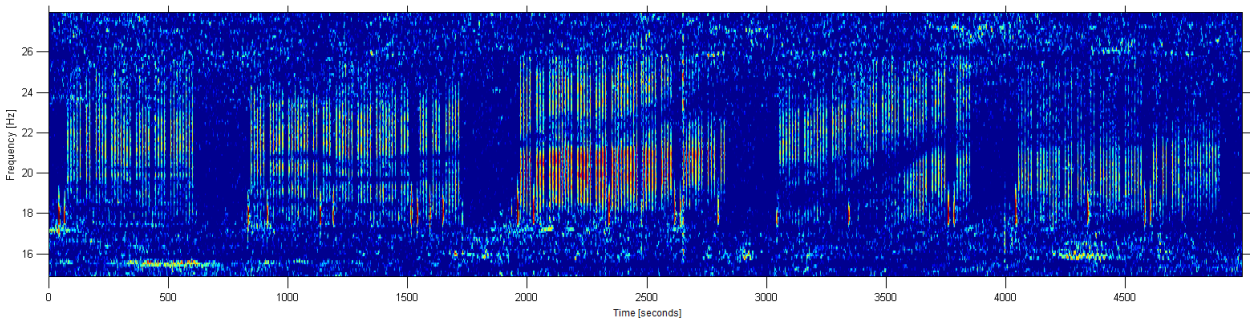

Figure 2. Spectrogram showing 01h23m19s of a fin whale bout where spectra consistent with frequency dependent interference patterns potentially due to LME were pronounced. The complete bout was produced during 3h20m. Back-beats (signals around 18 Hz) were also observed, but were not considered for the analysis. Spectrogram parameters: Frame size – 1024 samples, 95% overlap, Hanning window, equalized.

B. MEASURING CALL CHARACTERISTICS

Regular fin whale calls were identified using a modified normalized cross-correlation equation with a matched filter of the signal waveform (see Matias & Harris, 2015). Our detection routine also included the calculation of spectral cross-correlation, following the methodology of Mellinger & Clark (2000). A two-dimensional spectrogram synthetic kernel was constructed based on the sound of interest. We selected one day of the dataset when there were regular calls with high signal-to-noise ratio and high waveform cross-correlation values. The kernel base was derived by summing and averaging the spectra of these calls. The recorded time series was analyzed by its cross-correlation with the kernel. This produced a recognition function, which represented the likelihood at each point in time that the sound of interest was present. A threshold was then applied to both the waveform cross-correlation and the spectra function to obtain discrete detection events, times when the sound of interest was likely to be present. For each detection, several spectral and temporal features were computed based on Hatch & Clark (2004), namely frequency bandwidth, starting frequency, median frequency and signal duration. We assessed the variation of these features throughout the bout (including when the LME pattern was observed) by calculating derivatives of the smoothed original data. The resulting derivatives were smoothed again using an average smoothing method.

C. LME OBSERVATIONS

To better examine the spectral differences between calls, we extracted periods of silence between calls and plotted the calls as individual waveform traces side-by-side along the time axis (Fig. 3).

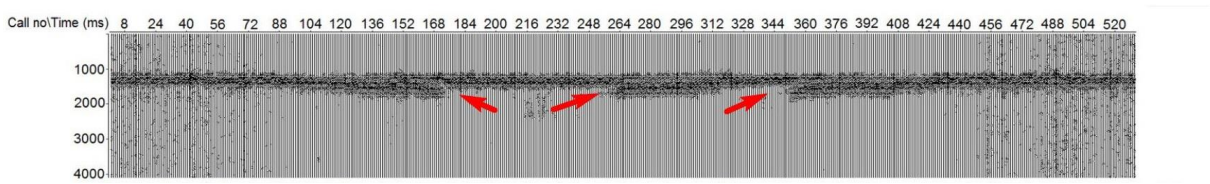

Figure 3. Individual trace of the waveform of each regular fin whale call of the bout (displayed vertically) through time.

We also created a composite spectrogram of the bout without the periods of silence for the vertical channel (Z channel) of the OBS (Fig. 4). Both the plotted waveforms and spectrogram clearly showed an interference pattern. Regular calls are highly stereotyped. Therefore, when they are produced in sequences both the waveforms and the composite spectrogram show a relatively stable stripe. However, call signals are changed when the surface-reflected path superimposes with the direct path of the call. This results in visible curved interference patterns both in the waveforms and spectrograms, which create a symmetrical "U" shape characteristic of the LME pattern (Hudson, 1983). In order to compare the observed interference pattern with modelled data we manually fitted curves by eye to the interference observed in our composite spectrogram. These curves represented our interpretation of the LME pattern. We kept image dimensions as constant as possible in order to avoid distortions of the interference patterns.

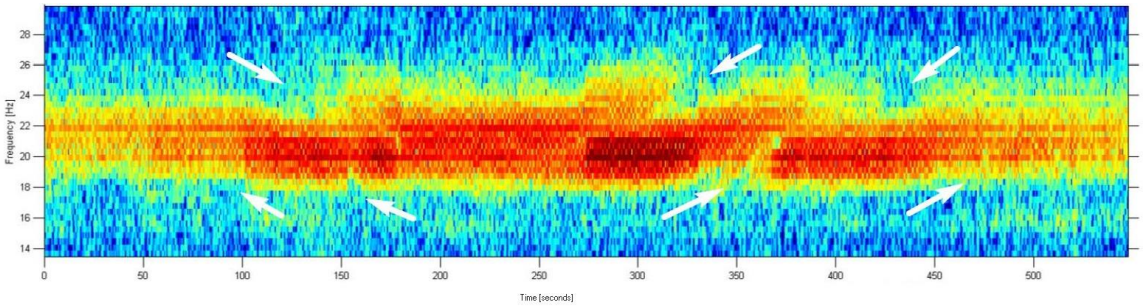

Figure 4. Composite spectrogram of the fin whale bout without periods of silence. Arrows show the features that are interpreted as LME interference patterns. Spectrogram parameters: Frame size – 256 samples, 95% overlap, Hanning window, not equalized.

We then simulated the effects of surface reflection on the shape of a regular call. For this, we developed MATLAB code where two synthetic identical pulses were added with an increasing delay that could be caused by a variable depth or by a variable distance between source and receiver. Figure 5 shows the synthetic signals side by side and we can see a similar interference pattern to the one in Fig. 3.

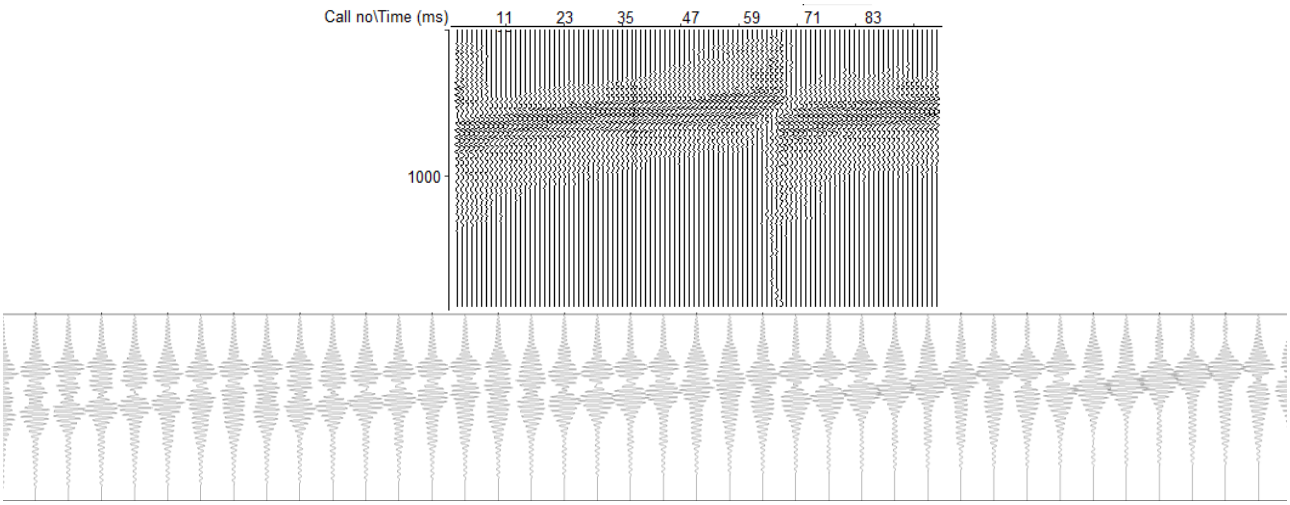

Figure 5. Superposition of two synthetic and identical fin whale regular calls with a decreasing delay, plotted side by side. Top) General pattern observed in a sequence of calls; Bottom) Zoom in to a group of calls.

D. SOUND SOURCE RANGE ESTIMATION

A variety of methods have been used to estimate ranges to vocalizing whales from OBS data, including the single-station method (SSM) (Harris et al., 2013), multipath-based techniques (Wilcock, 2012) and time difference of arrival (TDOA) approaches (Dunn & Hernandez, 2009). Range estimates of each regular call were obtained considering the difference between the arrival times of the direct signal and the multipath to the same OBS. The majority of the calls within the bout considered for this work were close to, or outside of, the critical range of the SSM (Matias & Harris, 2015) so the SSM was not applicable in this case. Multipath arrivals in this dataset had very small amplitudes, so we developed a methodology to enhance the signals using the seismic software SPW (Parallel Geoscience, 1999). The main processing steps were: i) Computation of the envelope of the waveforms using the Hilbert transform. This step transformed the regular call waveform into a smooth half-sine curve. ii) Signal filtering to enhance all envelopes with a ~0.8 s duration. iii) Since the direct path of the several calls of the bout were not perfectly aligned in time, we used the cross-correlation between each trace and a "pilot" trace to correct the small misalignments. This is a process identified as "residual statics" in seismic processing jargon. iv) Finally we applied an amplitude equalization by automatic gain control to facilitate the picking of the low amplitude multipaths of the regular calls. The arrival times for the direct path and multipath were picked as smooth continuous lines across the display (Fig. 6). The time difference between the direct path and multipath was converted to a range.

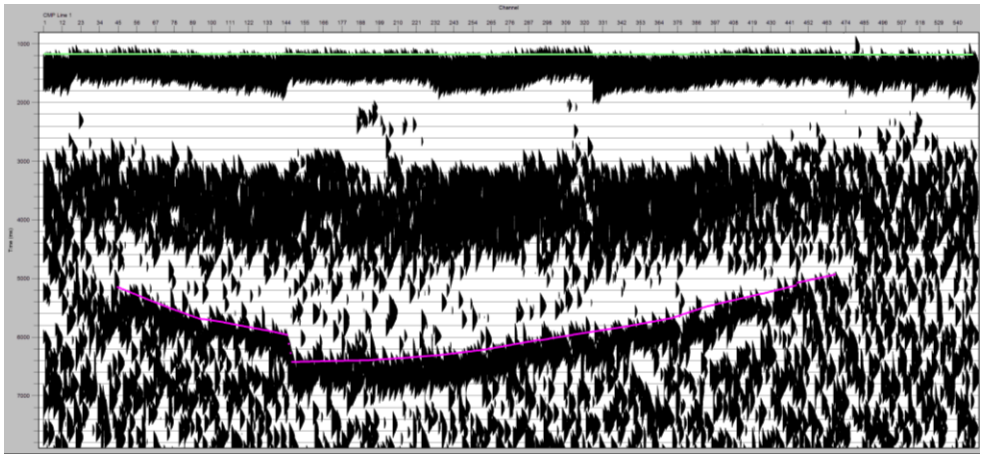

Figure 6. Display of the fin whale bout by SPW after computing the trace envelope and applying a band-pass filter and amplitude equalization. The green trace represents the direct pick times and the pink trace represents the multipath pick times.

All ranges of the fin whale calls in our dataset were well inside the range where LME was predicted to occur and far from the boundaries defined using Eqns. (1) and (2).

E. LME MODELLING

Since our fin whale acoustic dataset had a range estimate for each individual call, we used the LME to estimate the depth of the vocalizing whale. Considering a whale that produced sequences of regular calls near a smooth reflecting sea surface, the geometry of the LME is given in Fig. 7.

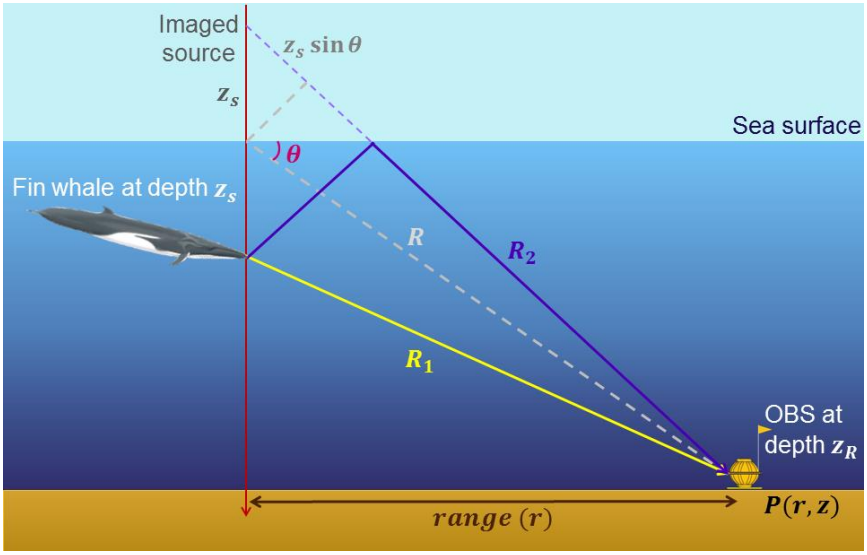

Figure 7. LME geometry with a fin whale as a sound source and the OBS as the receiver instrument. P(r,Z): Total amplitude of a signal at range r and received at depth Z. R_1 represents the direct signal path and R_2 shows the surface-reflected path.

The travel distances of the direct path, R_1, and the surface-reflected path, R_2, were calculated using Eq. $R0$ and 0 (Jensen et al., 2011):

$$R_1 = \sqrt{r^2 + (z_R - z_s)^2} \tag{3}$$

$$R_2 = \sqrt{r^2 + (Z_R + z_s)^2} \tag{4}$$

The total signal amplitude was calculated as the sum of the two sound sources. For a monochromatic wave, this amplitude is given by:

$$P(r,Z) = \frac{e^{ikR_1}e^{-\alpha R_1}}{R_1} + \mu\frac{e^{ikR_2}e^{-\alpha R_2}}{R_2} \tag{5}$$

Where k is the wave number of a monochromatic wave of wavelength λ (Eq. (6)),

$$k = \frac{2\pi}{\lambda} \tag{6}$$

and α is the frequency-dependent attenuation coefficient (Eq. (7)) (after Brekhovskikh & Lysanov, 1982):

$$\propto = 3.3 \times 10^{-3} + \frac{0.11f^2}{1+f^2} + \frac{44f^2}{4100+f^2} + 3.0 \times 10^{-4}f^2 \quad (f \text{ in } kHz) \tag{7}$$

The symbol μ represents the reflection coefficient at the surface. For pressure signal and a perfect reflector μ = -1. For particle velocity signal and a perfect reflector $\mu = 1$.

The transmission loss (TL) due to LME as applied to a fin whale call generated close to the surface and recorded at the sea bottom by an OBS was calculated using Eq. (8) and considering a reference pressure of P_{ref} = 1 µPa:

$$TL(r, Z) = -20log\left(\frac{P}{P_{ref}}\right) \quad (8)$$

For each trial source depth, we used Eq. (8) to compute the TL for all frequencies and ranges of interest and plotted the resulting synthetic spectrogram. TL models and figures were made using a modified version of the MATLAB code presented in Thompson (2009). The original code modelled TL using a regular range spacing and the altered code used our range estimates. Because fin whale calls have a limited frequency band, we applied a cosine taper between 18 and 24 Hz to generate synthetic calls. To make the figures more realistic we added some random noise to the modeled synthetic calls and adjusted the color scale to generate an image as close as possible to the observations. We developed synthetic transmission loss models for a sound source (Z_s) varying in depth between 10 and 500 m every 10 m. In order to compare the observed LME pattern with the modelled data, we overlaid the curves that represented the observed LME pattern on each synthetic spectrogram. Depth of the vocalizing whale was estimated by a visual assessment of the fit between the modelled data and the observed LME pattern considering: i) the whole bout; ii) only the most visible part of the interference pattern; and iii) the most visible part of the interference pattern with altered ranges. For the first analysis we assumed that the entire bout was produced at a constant depth and compared the complete interference pattern with the modelled data. To examine if the depth estimate of the first analysis was adequate we then estimated depth using only the most conspicuous features of the interference pattern. The use of multipaths to estimate range to the calls required a large amount of manual data selection i.e., identifying multipath arrivals. Therefore, the estimated ranges may contain some error. We assessed the potential effect of such error on the results by both increasing and decreasing the estimated ranges by 500 m and re-running the restricted analysis.

3. RESULTS

A. ANALYSIS OF LME CHANGES IN CALL CHARACTERISTICS

During the fin whale bout we interpreted an LME pattern that had three sections where there was a considerable change in the waveform of the regular calls: at calls #168, #260 and #350 (approximately) (Fig. 4). Those sections corresponded to three periods of the composite spectrogram where the curvatures of the LME pattern occurred: ~150, 300 and 350 seconds (Fig. 4). The smoothed derivative of the call features showed three main areas of change that coincided with the three sections of the LME pattern (Fig. 8). These areas were more pronounced in the signal quality related features. The spectral features were more variable but the smoothed derivative showed an accentuated change in the frequency bandwidth and median frequency. The large variation of the spectral features at the start and end of the bout coincided with the largest estimated ranges between the whale and the sensor and so is likely to be range-related.

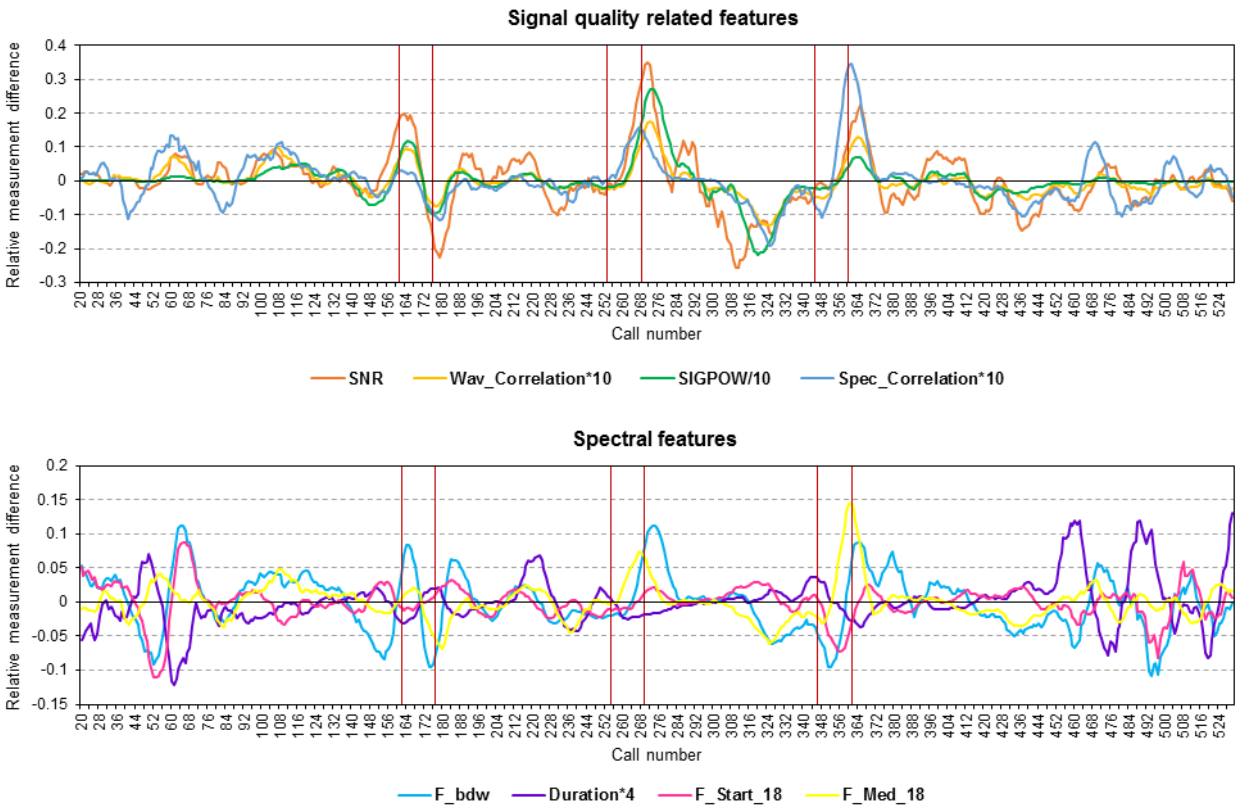

Figure 8. Smoothed derivative of the features of the regular fin whale calls. All features except signal-to-noise ratio (SNR) and frequency bandwidth (F_bdw) were scaled to fit in the same plot. Top) Signal quality related features: SNR – Signal-to-noise ratio; Wav_Correlation*10 – Waveform cross-correlation value multiplied by 10; SIGPOW/10 – Signal power divided by 10; Spec_Correlation*10 – Spectrogram correlation value multiplied by 10. Bottom) Spectral features: F_bdw – Frequency bandwidth; Duration*4 – Call duration multiplied by 4; F_Start_18 – Starting frequency, difference to 18 Hz; F_Med_18 – Median frequency, difference to 18 Hz. Vertical red lines represent the areas where the three curves of the interference pattern occurred. When the original data showed peaks the derivative is 0. When the curve of the derivative is positive there was an increasing tendency in the original data. If it is negative then there was a decreasing tendency.

B. INFERENCE OF DEPTH OF THE VOCALIZING WHALE

Even after the signal enhancement and additional processing treatment with the seismic software SPW not all multipaths of the calls could be identified. Therefore, further analysis of the LME was restricted to the individual traces where range could be estimated, and a new composite spectrogram was created (Fig. 9). Despite removing parts of the bout (e.g., Fig. 9 at 125 s), there was a clear symmetry in the pattern displayed (Fig. 9).

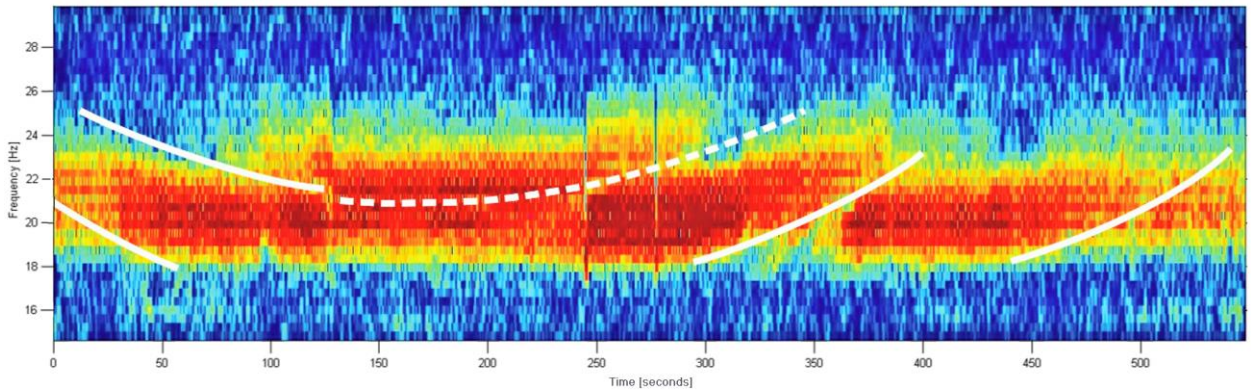

Figure 9. Composite spectrogram of the fin whale bout without regular calls that had no range estimate. White curves represent our interpretation of the LME interference pattern fitted by eye. Thick curves represent our most certain interpretation of the interference pattern. Dashed curve represent uncertainty in the continuity of the thick curve. Spectrogram parameters: Frame size – 256 samples, 95% overlap, Hanning window, not equalized.

The closest synthetic transmission loss models to our observations were the ones with a source depth between 330 and 350 m (Fig. 10, right). Models with shallower depths did not show very prominent interference patterns (Fig. 10, left).

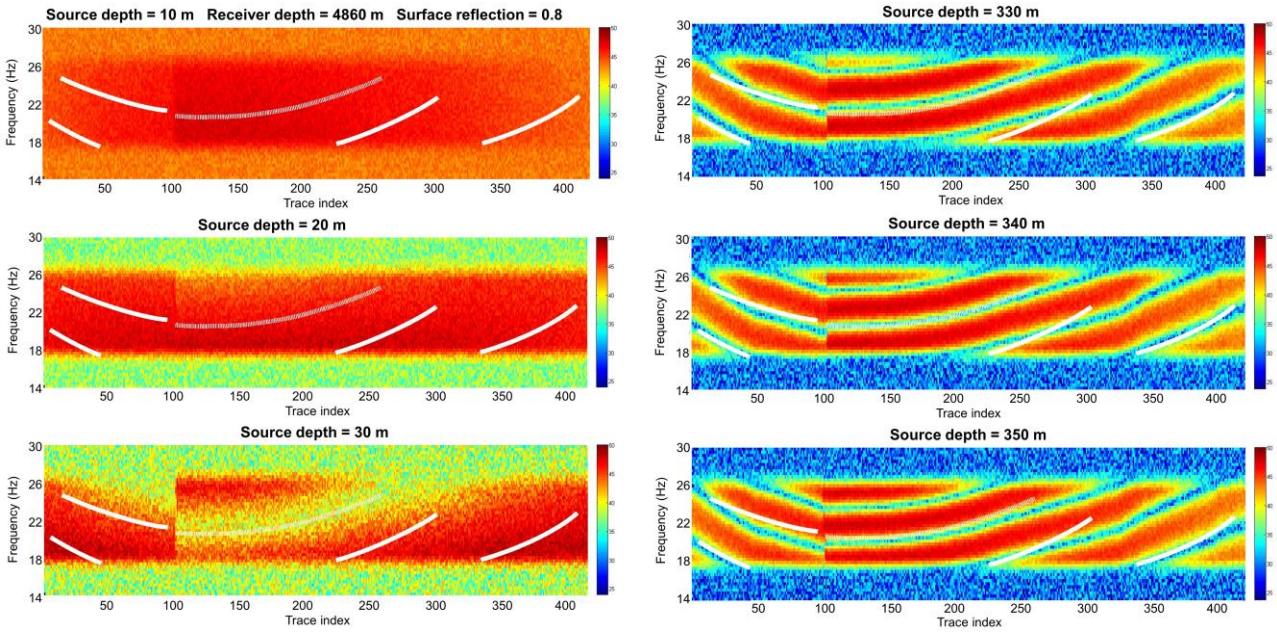

Figure 10. TL models for the LME with a varying source depth with the interference patterns identified in the composite spectrogram of the fin whale calls (white lines). Left from top to bottom) transmission loss models for source depths of 10, 20 and 30 m respectively; Right from top to bottom) transmission loss models for source depths of 330, 340 and 350 m respectively.

DEPTH ESTIMATION USING PART OF THE BOUT WITH THE MOST VISIBLE INTERFERENCE

In this second analysis, we estimated a vocalizing depth of ~40 m (Fig. 11, left). The model with an estimated depth of ~340 m no longer matched the observed lower curve (Fig. 11, right).

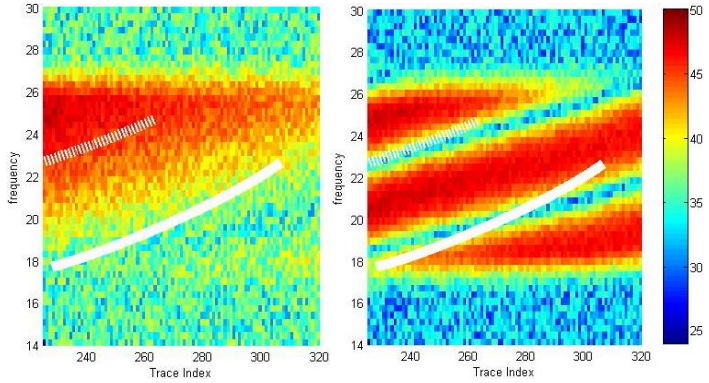

Figure 11. Best visual fit obtained by comparing the most prominent part of the interference pattern identified in the composite spectrogram of the fin whale calls (thick white line) with a transmission loss model for the LME with a source depth of 40 m (left) and 340 m (right). The dashed line starting at 23 Hz represented part of the interference pattern that was not considered for this part of the analysis because of its uncertainty.

The TL models calculated with altered ranges obtained for shallow source depths (up to 30 m) did not match the observed interference pattern. There were no significant changes in the interference patterns and the models with depths around 35-45 m retained the best fit (Fig. 12).

RANGES WITH +500 m

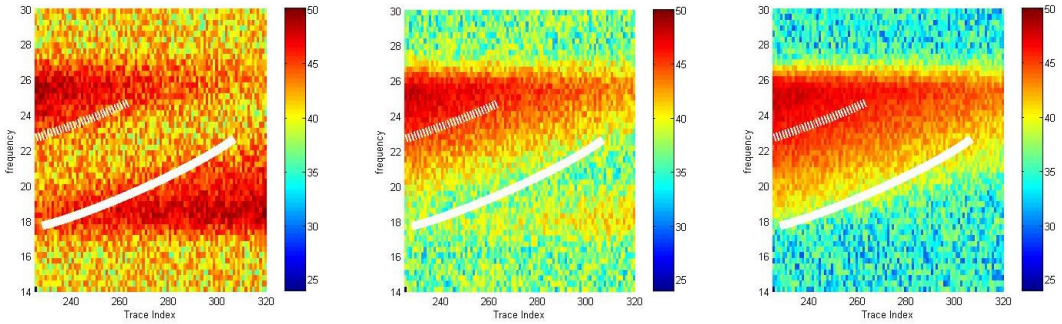

ORIGINAL RANGES

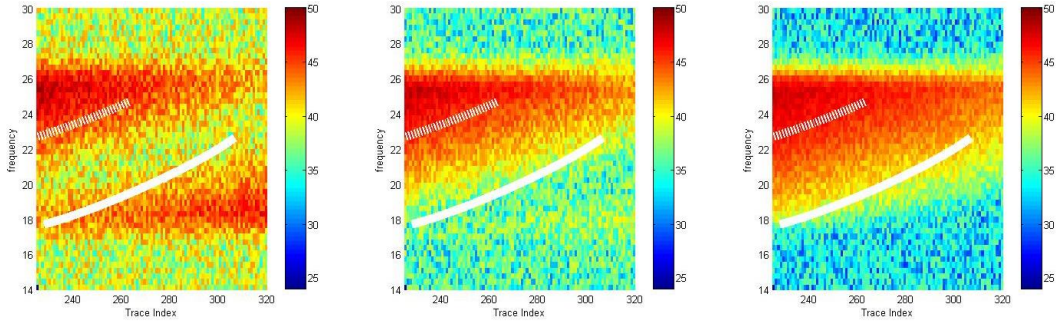

RANGES WITH -500 m

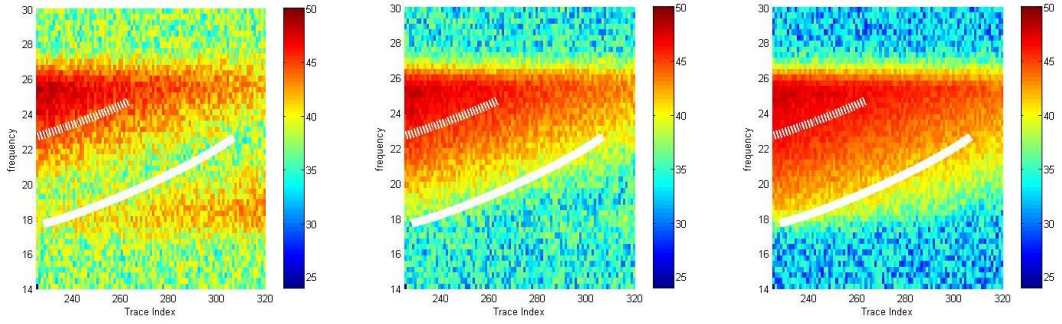

Figure 12. Best visual fit models obtained by comparing the most prominent part of the interference pattern (thick white lines) with a transmission loss model for the LME with a sound source depth of 35 m (left), 40 m (center) and 45 m (right) and a deviation of 500 m from the original estimated ranges. The dashed line represented part of the interference pattern that was not considered for this part of the analysis because of its uncertainty.

4. CONCLUSION

An understanding of acoustic propagation of biological signals in the ocean is crucial for studies of marine mammal sounds that rely on high quality and accurate characterization of the signals. Some characteristics associated with biological factors might be artefacts of propagation. For example, Premus & Spiesberger (1996) demonstrated that multipath propagation could explain the production of the 20-Hz doublets by fin whales in the Gulf of California. Measurement error might also occur due to interference caused by propagation. For example, inaccurate estimates of sound source levels have been related with the occurrence of LME (Charif et al., 2002). Here, accentuated changes in the frequency bandwidth and median frequency occurred at the same time as curved patterns in the spectrogram, characteristic of the "U" shape of the LME fringes. These results further suggest that LME can cause signal change and thus alter signal features that can be used to investigate spatiotemporal variation in stereotyped marine mammal vocalizations. The

frequency of occurrence and the extent of impact of the LME on studies that characterize signals of cetaceans remains unknown.

From our initial approach of estimating the depth of the entire bout we obtained a depth of ~340m, which is in agreement with the current knowledge of diving behavior of fin whales but not with their vocal activity. Aroyan et al. (2000) argue that the depth at which baleen whales call is limited by the volume of air required to produce the sound, a volume which decreases with depth due to increasing hydrostatic pressure. Fin whales can dive up to 470 m (Panigada et al., 1999) and the deepest dives are typically feeding dives (Goldbogen et al., 2006). However, vocal activity of fin whales is thought to occur at shallower depths. Tagged fin whales off Southern California showed that individuals called at depths up to approximately 15-20 m (Stimpert et al., 2015). Behavioral descriptions from Watkins et al. (1987) reports depths of ~50 m for vocalizing whales. For the 340m estimated vocalizing depth, we assumed a constant depth for the entire bout, which is likely to be an unrealistic assumption. When we estimated the depth of only the most visible interference pattern, the best fit model was the one with depths around 35-45 m, which is in the range of previously estimated vocalizing depths for fin whales. None of our models supported a depth between 10-30 m.

There were sources of potential bias and uncertainty in these analyses that require discussion. Firstly, our transmission loss models depended on the estimated ranges of the calls. All ranges of the fin whale calls in our dataset were well inside the range where LME was predicted to occur and far from the boundaries defined using Eqns (1) and (2). A bias in the estimated ranges could occur because of small processing errors in the manual part of the methodology. However, our tests with a 500 m deviation in range showed that TL models did not change significantly. These results suggest that our models may tolerate some level of measurement error in the range estimates, though a more thorough investigation is required. Secondly, the interference curves were identified by eye and no quantitative model fitting routine was implemented to find the model with the best fit to the observed interference patterns. A more developed analysis with automated identification of interference curves and model fit, in addition to a review of the transmission loss model, will be undertaken in order to verify our results about the LME in fin whale calls and its use to infer the depth of vocalizing whales.

ACKNOWLEDGMENTS

The acoustic data were collected for the NEAREST project, on behalf of the EU Specific Programme “Integrating and Strengthening the European Research Area,” Sub-Priority 1.1.6.3, “Global Change and Ecosystems,” Contract No. 037110. The data analysis is part of the Ph.D thesis by A.P, which is funded by the Portuguese Foundation for Science and Technology (Fundação para a Ciência e Tecnologia; SFRH/BD/52554/2014). We would like to thank the organizing committee of the “The Effects of Noise on Aquatic Life” conference for the opportunity to publish the work presented at the conference. We would also like to thank Francisco Martinho for the fin whale illustration used in Fig. 7.

REFERENCES

Aroyan, J. L., McDonald, M. A., Webb, S. C., Hildebrand, J. A., Clark, D., Laitman, J. T., and Reidenberg, J. S. (**2000**). “Acoustic models of sound production and propagation,” in *Hearing by Whales and Dolphins*. (edited by W. W. L. Au, A. N. Popper, and R. R. Fay (Springer, New York), pp. 409-469.

Brekhovskikh, L., and Lysanov, Y. (**1982**). *Fundamentals of Ocean Acoustics* (Springer-Verlag, Berlin).

Castellote, M., Clark, C. W., and Lammers, M. O. (**2011**). "Fin whale (*Balaenoptera physalus*) population identity in the western Mediterranean Sea," Marine Mammal Sci. **28**, 325–344.

Charif, R.A., Mellinger, D.K., Dunsmore, K.J., Fristrup, K. M., and Clark, C. W. (**2002**). "Estimated sound source levels of fin whale (*Balaenoptera physalus*) vocalizations: adjustments for surface interference," Marine Mammal Sci. **18**, 81–98.

Clark, C. W., Borsani, J. F., and Notarbartolo-di-Sciara, G. (**2002**). "Vocal activity of fin whales, *Balaenoptera physalus*, in the Ligurian Sea," Marine Mammal Sci. **18**, 281–285.

Croll, D. A., Acevedo-Gutiérrez, A., Tershy, B. R., and Urbán-Ramírez, J. (**2001**). "The diving behavior of blue and fin whales: is dive duration shorter than expected based on oxygen stores?," Comp. Biochem. Physiol., Part A Mol. Integr. Physiol. **129**, 797–809.

Delarue, J., Todd, S., Parijs, S. V., and Iorio, L. D. (**2009**). "Geographic variation in Northwest Atlantic fin whale (*Balaenoptera physalus*) song: Implications for stock structure assessment," J. Acoust. Soc. Am. **125**, 1774–1782.

Dunn, R. A., and Hernandez, O. (**2009**). "Tracking blue whales in the eastern tropical Pacific with an ocean-bottom seismometer and hydrophone array," J. Acoust. Soc. Am. **126**, 1084–1094.

Etter, P. C. (**2013**). *Underwater Acoustic Modeling and Simulation* (CRC Press, Taylor & Francis Group, Boca Raton, FL).

Fristrup, K. M., and Watkins, W. A. (**1993**). "Marine animal sound classification". Woods Hole Oceanographic Institution Technical Report WHOI-94- 13. 29 pp.

Goldbogen, J. A., Calambokidis, J., Shadwick, R. E., Oleson, E. M., McDonald, M. A., and Hildebrand, J. A. (**2006**). "Kinematics of foraging dives and lunge-feeding in fin whales," J. Exp. Biol. **209**, 1231–1244.

Harris, D., Matias, L., Thomas, L., Harwood, J., and Geissler, W. H. (**2013**). "Applying distance sampling to fin whale calls recorded by single seismic instruments in the Northeast Atlantic," J. Acoust. Soc. Am. **134**, 3522–3535.

Hatch, L. T. and Clark, C. W. (**2004**). "Acoustic differentiation between fin whales in both the North Atlantic and North Pacific Oceans, and integration with genetic estimates of divergence," Paper presented to the IWC Scientific Committee, Sorrento, Italy, July, Paper No. SC/56/SD6, pp. 1–37.

Hudson, R. F. (**1983**). "A Horizontal Range vs. Depth Solution of Sound Source Position under General Sound Velocity Conditions using the Lloyd's Mirror Interference Pattern," M.Sc. thesis, Naval Postgraduate School.

Jensen, F. B., Kuperman, W. A., Porter, M. B., and Schmidt, H. (**2011**). *Computational Ocean Acoustics*. (Springer Science+Business Media, LLC, New York).

MathWorks. (2010). MATLAB (Version 7.10) [Computer Software]. The Mathworks, Inc., Natick, MA.

Matias, L., and Harris, D. (**2015**). "A single-station method for the detection, classification and location of fin whale calls using ocean-bottom seismic stations," J. Acoust. Soc. Am.**138**, 504–520.

McDonald, M. A., Mesnick, S. L., and Hildebrand, J. A. (**2006**). "Biogeographic characterisation of blue whale songs worldwide: Using song to identify populations," J. Cetacean Res. Manage. **8**, 55–65.

Mellinger, D. K., and Clark, C. W. (**2000**). "Recognizing transient low-frequency whale sounds by spectrogram correlation," J. Acoust. Soc. Am. **107**, 3518–3529.

Panigada, S., Zanardelli, M., Canese, S. and Jahoda, M. (**1999**). "How deep can baleen whales dive?," Mar. Ecol. Prog. Ser. **187**, 309–311.

Premus, V., and Spiesberger, J. L. (**1997**). "Can acoustic multipath explain finback (*B. physalus*) 20-Hz doublets in shallow water?" J. Acoust. Soc. Am., **101**, 1127-1138.

Širović, A., Williams, L. N., Kerosky, S. M., Wiggins, S. M., and Hildebrand, J. A. (**2013**) "Temporal separation of two fin whale call types across the eastern North Pacific," Mar. Biol. **160**, 47–57.

Soule, D.C., and Wilcock, W. S. D. (**2012**). "Fin whale tracks recorded by a seismic network on the Juan de Fuca Ridge, Northeast Pacific Ocean," J. Acoust. Soc. Am. **133**, 1751–1761.

Stimpert, A. K., DeRuiter, S. L., Falcone, E. A., Joseph, J., Douglas, A. B., Moretti, D. J., Friedlaender, A. S., Calambokidis, J., Gailey, G., Tyack, P. L., and Goldbogen, J. A. (**2015**). "Sound production and associated behavior of tagged fin whales (*Balaenoptera physalus*) in the Southern California Bight," Anim Biotelemetry **3**: 23.

Thompson, S. R. (**2009**). "Sound propagation considerations for a deep-ocean acoustic network," M.Sc. thesis, Naval Postgraduate School.

Watkins, W. A., Tyack, P., Moore, K. E., and Bird, J. E. (**1987**). "The 20-Hz signals of finback whales (*Balaenoptera physalus*)," J. Acoust. Soc. Am. **82**, 1901–1912.

Wiggins, S. M., Roch, M. A., and Hildebrand, J. A. (**2010**). "TRITON software package: Analyzing large passive acoustic monitoring data sets using MATLAB," J. Acoust. Soc. Am. **128**, 2299.

Wilcock, W. S. D. (**2012**). "Tracking fin whales in the northeast Pacific Ocean with a seafloor seismic network," J. Acoust. Soc. Am. **132**, 2408–2419.